

ENCIT-2018-0822

PERFORMANCE CONTROL AND ANALYSIS OF A PARABOLIC SOLAR CONCENTRATOR USED FOR WATER HEATING

Lino Wagner Castelo Branco Portela

Departamento de Engenharia Mecânica, Universidade Federal do Ceará – UFC, Curso de Pós-Graduação em Engenharia Mecânica, Campus do Pici – CEP: 60455-760 – Fortaleza-CE, Brasil
linowcbp@gmail.com

Erilson de Sousa Barbosa

Universidade Federal do Piauí – UFPI, Laboratório de Energias Renováveis – LER, Curso de Engenharia Mecânica, Campus Universitário Ministro Petrônio Portella – Bairro Ininga – CEP: 64049-550 – Teresina-PI, Brasil
erilson@ufpi.edu.br

Ana Fabíola Leite Almeida

Departamento de Engenharia Mecânica, Universidade Federal do Ceará – UFC, Curso de Pós-Graduação em Engenharia Mecânica, Campus do Pici – CEP: 60455-760 – Fortaleza-CE, Brasil
anfaleal@yahoo.com.br

Ricardo Silva Agostinho

Universidade Federal do Piauí – UFPI, Laboratório de Energias Renováveis – LER, Curso de Engenharia Mecânica, Campus Universitário Ministro Petrônio Portella – Bairro Ininga – CEP: 64049-550 – Teresina-PI, Brasil
ricardosilva130@hotmail.com

Abstract. *Parabolic solar concentrators are commonly used in solar thermal systems in which the working fluid reaches higher temperatures than can be obtained in flat plate solar collectors. The parabolic solar concentrator (CSP) requires a control system that positions itself properly throughout the day in relation to the sun in order to collect the direct solar radiation and to concentrate it in the tube located in the focus of the parabolic trough. This study aims to present a fluid analysis in a CSP controlled by a microcontrolled electronic system, as well as the analysis of its performance. The control system consists of an Arduino electronic board and sensors of the type LDR (Light Dependent Resistors) that varies its resistance according to the incidence of luminosity in its surface and are responsible for seeking better levels of radiation. As a validation of the operation of the control system, the measurements of temperatures at external points of the wall of the copper tube receiving the concentrated solar radiation are presented; also the inlet and outlet of the water fluid and the measurement of solar radiation.*

Keywords: *Parabolic Solar Concentrator, Control System, Solar radiation, Temperature.*

1. INTRODUCTION

Solar energy can be converted into thermal energy in different forms. Therefore, it can be an alternative to the consumption of conventional energies, such as those derived from petroleum and coal.

The Brazilian territory is among those that present enormous potential for the exploration of solar radiation. Despite this, the use of this technology and its development is still very low. In 2015, the Ministry of Mines and Energy (MME) announced that the planning for the next decade for the installed power of electricity from the sun will represent almost 4% of the total Brazilian power of 2024. Currently, the source is responsible for 0,02% of the country's electric power.

In recent years in the state of Piauí, the government, educational institutions and private companies have awakened to the energy potential of this state (ENEL, 2016). In this region of Brazil, there is still a greater trend in the use of photovoltaic panels for low-level electricity generation, especially in rural regions, although these systems still have a high financial cost of implementation.

CSPs have several applications ranging from water heating to industrial processes to the generation of electricity in the order of tens of Mega Watts. Werner (2006) found that in 32 countries in Europe involved in research, 57% of industrial heating processes required fluids at temperatures below 400 °C. Therefore, the use of small parabolic solar concentrators can represent a saving of electrical energy relevant to the industrial sector.

Water vapor is used as a means of generating, transporting and using energy from the earliest stages of industrial development. Since in this physical state, it presents high energy content per unit mass and volume, besides being the most abundant compound on Earth and, therefore, easy to obtain and low cost (BIZZO, 2003). In this way, the importance of studying the vapor characteristics that these concentrators are capable of producing from the use of solar energy is considerable.

The state of Piauí is known nationally for having, throughout the year, the sensation of high rates of solar radiation, high temperatures and low relative humidity of the air. These three factors together are presented as a very favorable condition for the use of parabolic solar concentrators. According to Martins et al. (2005), the state of Piauí is part of a group of regions that present the highest values of direct solar radiation and in the inclined plane.

2. THE PARABOLIC SOLAR CONCENTRATOR

The parabolic solar concentrator in which the tracking system was fixed was developed at the Renewable Energy Laboratory of the Federal University of Piauí. The structure of the solar collector was fabricated with square and rectangular carbon steel profiles and a 0.8 mm thick AISI 430 mirrored stainless steel plate was used as the reflecting surface. At the center of the parabolic trough was a copper tube with a diameter of $\frac{1}{2}$ ". The opening of the concentrator is 900 mm wide and 1800 mm long.

Figure 1 shows the image of the parabolic solar concentrator.



Figure 1. Parabolic Concentrator. Source: Own authorship, 2017.

For transmission of motion and torque between the stepper motor type actuator and the hub structure, a mechanical system was used consisting of toothed belt and synchronizing pulleys. The system can be seen in Figure 2.



Figure 2. Mechanical transmission system. Source: Own authorship, 2017.

3. THE SOLAR TRACKING SYSTEM

To track the sun throughout the day, a tracking system was developed which was attached to the parabolic concentrator structure. This system is controlled by an Arduino Mega 2560 R3 microcontroller. Among its main features: 54 digital input / output pins, 16 analog inputs, 4 serial hardware ports and USB cable connection (ARDUINO, 2017). In Figure 3 is the image of the Arduino board.



Figure 3. Arduino Mega Microcontroller 2560 R3. Source: Arduino, 2017.

The light sensor module used consists of two NORPS-12 sensors of the type LDR (Light Dependent Resistors). In the datasheet of this component it is defined as a CdS photoconductive cell, which has a spectral response similar to that of the human eye. According to Dally et al. (1993), the LDR is made from semiconductor materials, usually cadmium sulphide (CdS) or cadmium selenide (CdSe), as these have an excellent photoconductive response. Figure 4 illustrates the surface of an LDR.

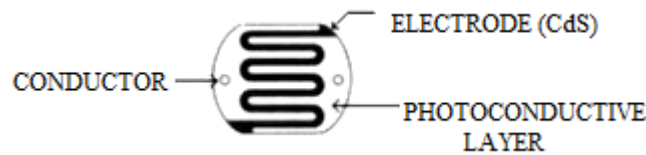


Figure 4. Surface of an LDR. Source: Adapted from Dally et al, 1993.

The module with the LDR sensors has the function of sending to the control board the information necessary to trace the solar radiation level. These sensors have a variable resistance according to the luminous intensity that affects their surface (BARBOSA, 2009).

Figure 5 shows the relationship between the electrical resistance measured in ohm of the NORPS-12 LDR as a function of the variation of the characteristic illumination index.

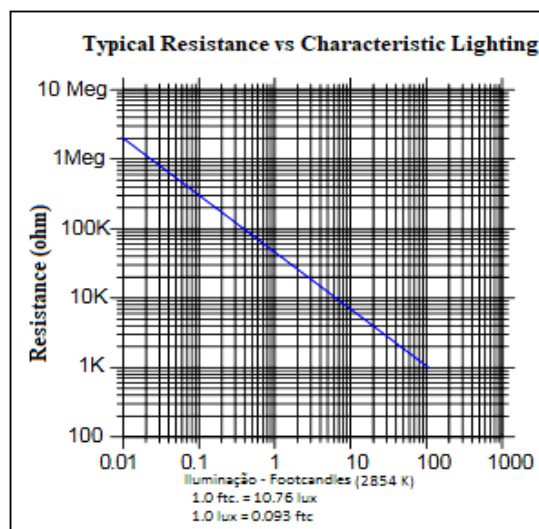


Figure 5. Variation of the electrical resistance of the LDR in function of the variation of the luminosity measured in footcandle. Source: Adapted from Silonex Inc., 2017.

The main advantage of LDR sensors is the generation of the signal in the magnitude of the reference voltage of the microcontroller, in addition to its low cost. On the other hand, the disadvantage of its use is its high sensitivity to small variations in brightness. However, on an experimental basis, it was possible to verify the behavior of these variations, and then add to the scheduling of the tracking system. Figure 6 shows the sensor module with LDRs.

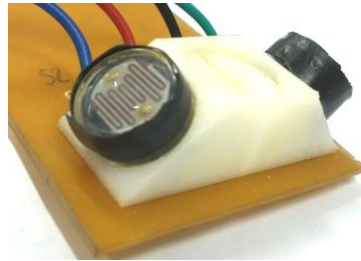


Figure 6. Sensor module with LDRs. Source: Own authorship, 2017.

The LDRs located in the inclined planes (45° in relation to the base) are responsible for providing the electrical resistance that will determine in which direction the concentrator should rotate.

4. SENSORS AND THE DATA COLLECTION INSTRUMENTATION

Temperature data were collected on the outer wall of the copper tube located at the parabolic trough focus, and solar radiation data. In the data collection of temperature, were used type K thermocouples, they have a reading range of -270°C to 1372°C ; analog output between 6.458 mV and 54.886 mV. In addition, they are formed by two metallic wires, Nickel and Chromium, which were attached at their end and placed in contact with the outer wall of the tube. Figure 7 shows this type of thermocouple.

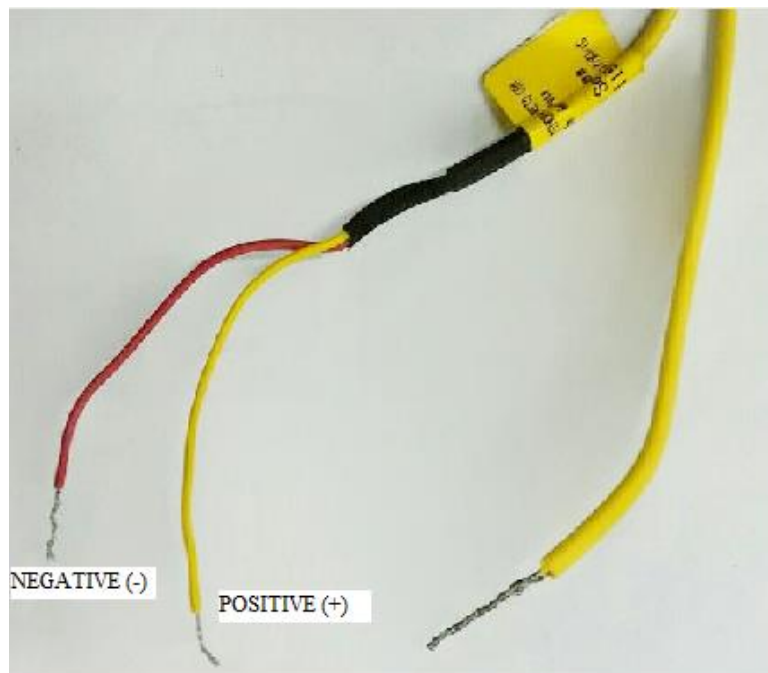


Figure 7. Thermocouple type K sensor. Source: Own authorship, 2017.

In the acquisition of solar radiation data, a KIMO™ piranometer, model CR 110, was used, with a measurement range of 0 to 1500 W/m^2 , a spectral response of 400 to 1100 nm, a remote sensor with a 2000 mm cable with a photovoltaic sensor with UV filter, electronics protected by ABS housing with IP65 degree of protection. It consumes between 0-10 V or 4-20 mA (KIMOTM, 2017). According to NBR IEC 60529: 2017, this protection is against dust and also water jets. In Figure 8 is the model of the sensor used.



Figure 8. Solar radiation sensor model CR 110. Source: KIMO™, 2017.

The registry and monitoring of these variables were done through a data controller of the brand Contemp™, model A202. This datalogger is characterized by eight configurable universal inputs. Its computational interface, MasterLogger A202, is a supervisory system that allowed to monitor and characterize the data that were provided by the pyranometer and the thermocouples in an electrical voltage unit.

This software (MasterLogger A202) has a simple interface, and allows interaction with measured quantities, including graphics and alarms. In addition, the computational interface has the functionality of generating PDF report, containing tables and graphs of the data in the historical or logger mode, data analysis with information of minimum, maximum and average value of each channel, as well as the personalization of fields and report logo (CONTEMP™, 2017).

With this, graphs were developed relating the variables of the system, making possible the analyzes and conclusions. Figure 9 shows the A202 datalogger used in this experiment.

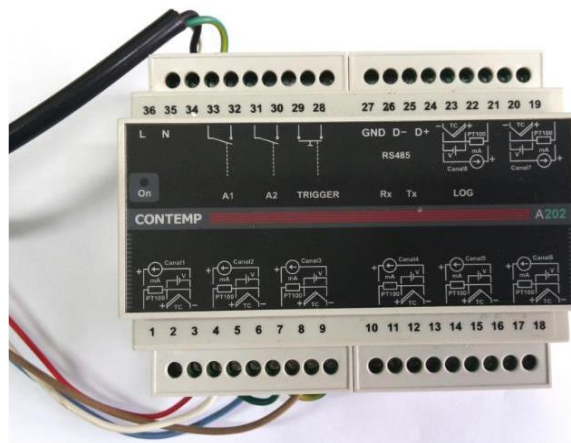


Figure 9. Datalogger Contemp™, model A202. Source: Own authorship, 2017.

5. RESULTS AND DISCUSSION

To verify the performance of the parabolic solar concentrator and its tracking system, solar radiation, temperature on the external surface of the absorber tube and temperature of the fluid used (water) were collected.

In the temperature measurement, five thermocouples were used. The first thermocouple was used to measure the water temperature at the inlet of the tube, being placed inside the hose that fed the system; another three were attached together to the outer surface of the tube, and the tube temperature was measured; already the fifth one, was placed in the exit of the system with the purpose of measuring the exit temperature of the water. As for measuring the incidence of solar radiation, the pyranometer sensor was fixed to the lateral surface of the parabolic trough.

Figure 10 shows how the thermocouples were arranged; Figure 11 shows the pyranometer.



Figure 10. Location of the thermocouple sensors. Source: Own authorship, 2017.



Figure 11. Location of the pyranometer sensor. Source: Own authorship, 2017.

The behavior of the concentrator was analyzed in two different situations, in two days. On the two days of temperature and solar radiation measurement, both experiments were carried out in a permanent regime. The water flow rate on the first day was approximately $0.04 \times 10^{-4} \text{ m}^3 \cdot \text{s}^{-1}$.

Figure 12 shows the variation of the temperature of the absorber tube with the variation of solar radiation. This experiment was carried out on November 20, 2017. The graph presented in Figure 13 shows the temperature measurement of the water entering the concentrator and the variation of the temperature of the water leaving the solar radiation.

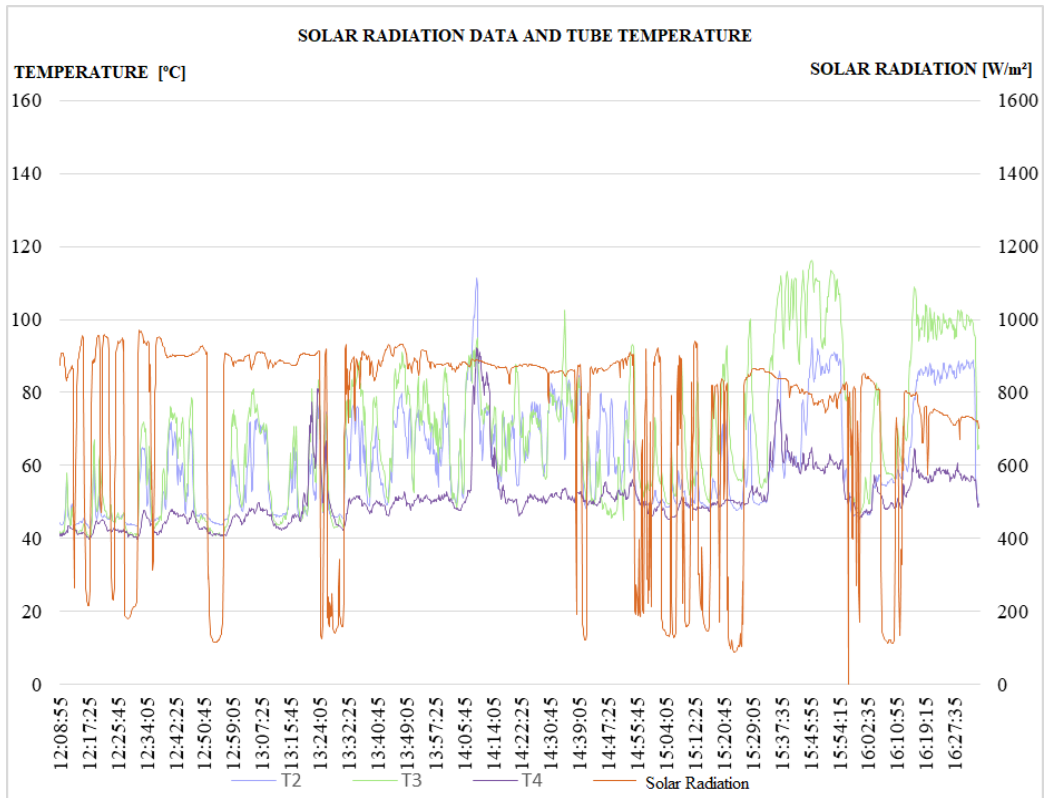


Figure 12. Distribution of solar radiation and absorber tube temperature, performed on 11/20/2017. Source: Own authorship, 2017.

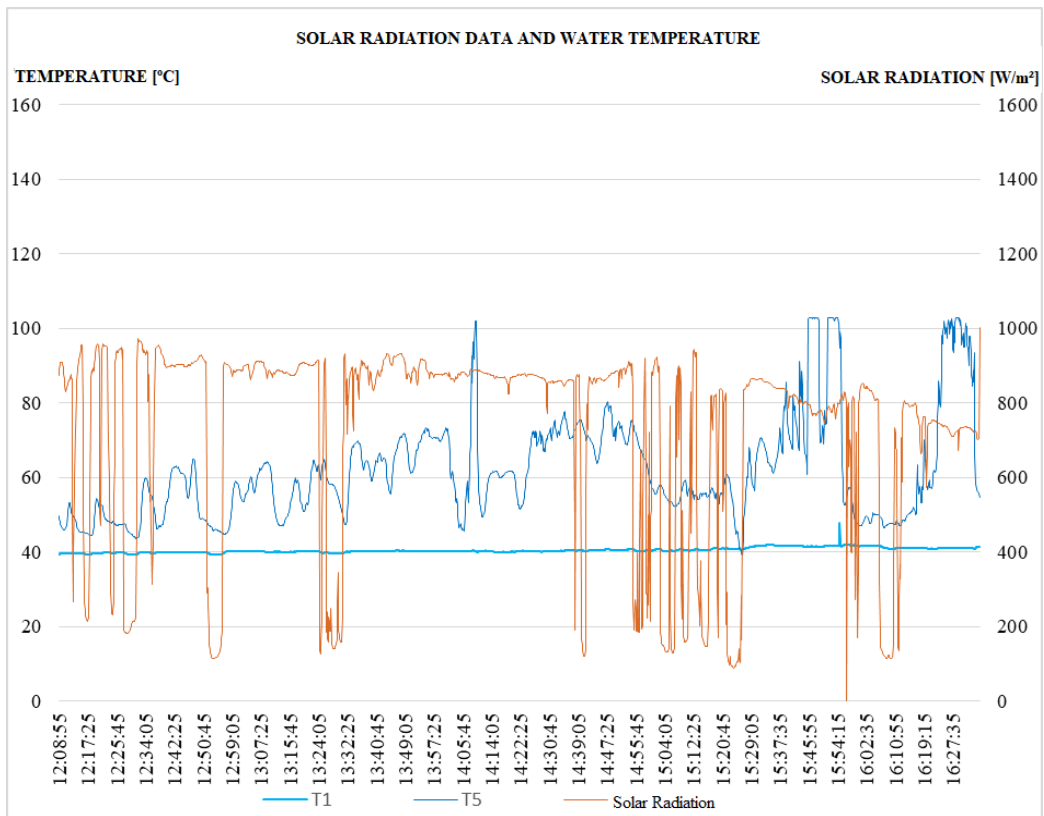
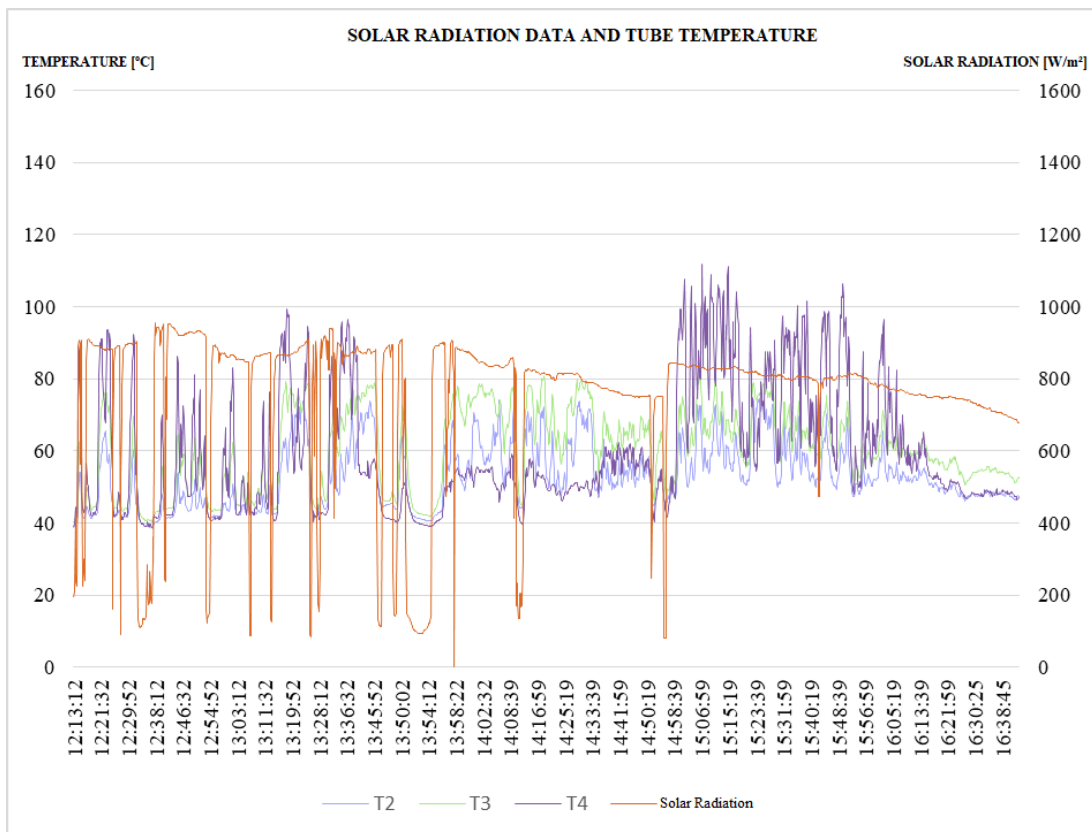


Figure 13. Distribution of solar radiation and water inlet and outlet temperature, performed on 11/20/2017. Source: Own authorship, 2017.

In these graphs, it is possible to perceive the presence of high solar radiation indices. We can see that while the sky remained low, the incidence of solar radiation was above 800 W/m^2 . During this period, at various times, it reached more than 900 W/m^2 . Regarding the temperature in the tube, the highest measured temperature was 115.4°C , at which point the water temperature was above 100°C - leaving its liquid state and passing to steam. It can also be observed that this type of collector presents / displays inferior performance when the presence of clouds is present. This can be seen in the graph at different intervals, such as in the period between 12h50min and 12h58min, where tube and fluid temperatures have declined considerably.

On the second day, with a slightly lower water flow, the highest temperature measured in the tube was 108.8°C , at that point the water temperature reached close to 80°C ; remaining in the liquid state. This variation may have occurred due to the increase in water flow and also to the incidence of wind, although the radiation indexes, in relation to the experiment carried out the previous day (11/20/2017), were very close.

Figure 14 shows the distribution of solar radiation and temperature of the absorber tube, experiment performed on November 21, 2017; in Figure 15 the solar radiation and water inlet and outlet temperature.



**Figure 14. Distribution of solar radiation and temperature of the absorber tube, performed on 11/21/2017.
Source: Own authorship, 2017.**

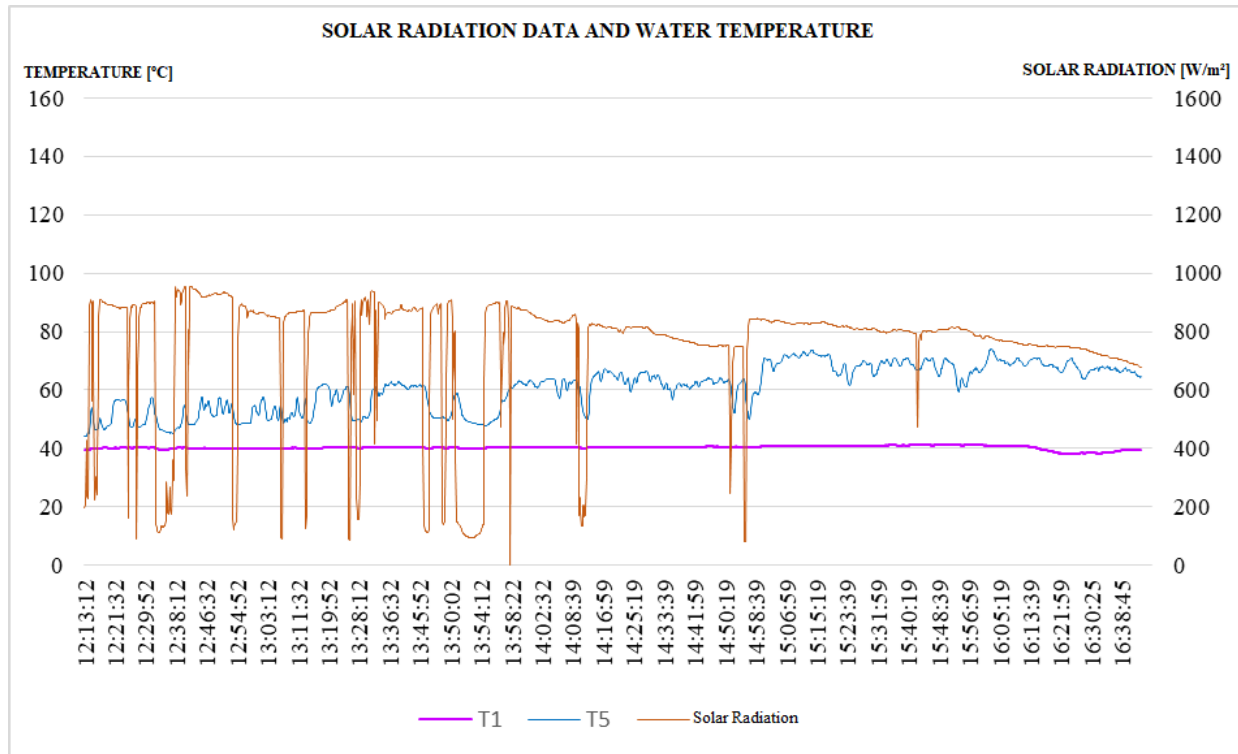


Figure 15. Distribution of solar radiation and water inlet and outlet temperature, performed on 11/21/2017.
Source: Own authorship, 2017.

6. CONCLUSION

From the data obtained from the temperature of the tube located in the parabolic trough and the water (entrance and exit), as well as verifying the variation of these temperatures with the variation of the level of incident solar radiation, it was verified that the parabolic solar concentrator and its tracking system presented satisfactory performance considering that it was able to transform the liquid water into steam at a constant flow rate. It was also possible to verify that the tube, despite being exposed to the environment, suffered low heat loss due to the convection phenomenon. This is due to the recognized low wind speed that is common in the city of Teresina, Piauí.

In relation to the control system used, it was observed that its operation was adequate by observing the luminosity incident on the tube and the high temperature values measured on the surface of the tube.

7. ACKNOWLEDGEMENTS

We thank the National Council for Scientific and Technological Development (CNPq) for the promotion of the research through the publication N° 18/2013 MCTI / CNPq / SPM-PR / Petrobras - Girls and Young People Making Exact Sciences, Engineering and Computing.

8. REFERENCES

- Ministério de Minas e Energia. Fonte solar será responsável por 7 mil MW na matriz elétrica até 2024. Brasília: MME, 2015. Disponível em: <<https://goo.gl/rb7AUr>> Acesso em: 09 jun. 2017.
- ENEL. Enel starts construction of latin americas largest solar power plant in brazil. Roma, 2016. Disponível em: <<https://www.enelgreenpower.com/en/media/press/d201607-enel-starts-construction-of-latin-americas-largest-solar-power-plant-in-brazil.html>>. Acesso em: 06 jun. 2017.
- Werner, S. The European heat market, work package 1. Final Rep. Brussels: Euroheat & Power, 2006.
- Bizzo, W.A. Geração, Distribuição e Utilização de Vapor. Campinas: UNICAMP, 2003.
- Martins, F.R.; Pereira, E.B.; Abreu, S.L.; Colle, S. Mapas de irradiação solar para o Brasil – Resultados do Projeto SWERA. Anais XII Simpósio Brasileiro de Sensoriamento Remoto, Goiânia, Brasil, 16-21 abril 2005, INPE, pp. 3137-3145.
- ARDUINO. Arduino Mega 2560 Rev3. Disponível em: <<https://store.arduino.cc/usa/arduino-mega-2560-rev3>>. Acesso em: 08 nov. 2017.

- Dally, J.W., Rilley, W.F., McConnel, K.G. Instrumentation for Engineering Measurements. 2^a. Ed. John Wiley & Sons, Inc. 1980.
- Barbosa, E.S. Desenvolvimento de um Sistema de Controle para Concentradores Parabólicos de Baixo Custo Aplicados à Refrigeração. Dissertação de mestrado - Universidade Federal do Ceará, Fortaleza, Brasil, 97p, 2009.
- Silonex, I. Norps-12 Datasheet. Disponível em: <<http://www.alldatasheet.com/datasheet-pdf/pdf/205862/SILONEX/NORPS-12.html>>. Acesso em: 08 nov. 2017.
- KIMOTM. CR 110: Capteur/transmetteur de rayonnement solaire. Disponível em: <<http://www.kimo.fr/fr/capteur/cr-110>>. Acesso em: 08 nov. 2017.
- Associação Brasileira de Normas Técnicas. NBR IEC 60529: Graus de proteção providos por invólucros (Códigos IP). Rio de Janeiro, 2017. Disponível em: <<http://www.abntcatalogo.com.br/norma.aspx?ID=369851#>>. Acesso em: 19 nov. 2017.
- CONTEMP. Medição, Controle e Monitoramento de Processos Industriais. Disponível em: <<http://www.contemp.com.br/produto/data-logger/>>. Acesso em: 14 nov. 2017.

9. RESPONSIBILITY NOTICE

The author(s) is (are) the only responsible for the printed material included in this paper.